Available online at www.sciencedirect.com
ScienceDirect
Acta Materialia 54 (2006) 4693–4698
Acta MATERIALIA
www.actamat-journals.com

# Dynamic magnetization process of nanocrystalline tape wound cores with transverse field-induced anisotropy

Sybille Flohrer [a,*], Rudolf Schäfer [a], Jeffrey McCord [a], Stefan Roth [a], Ludwig Schultz [a], Fausto Fiorillo [b], Wulf Günther [c], Giselher Herzer [c]

[a] *IFW Dresden, Institute for Metallic Materials, P.O. Box 270116, D-01171 Dresden, Germany*
[b] *Istituto Nazionale di Ricerca Metrologica INRIM, Strada delle Cacce 91, 10135 Torino, Italy*
[c] *Vacuumschmelze GmbH & Co. KG, Grüner Weg 37, D-63450 Hanau, Germany*

Received 20 March 2006; received in revised form 22 April 2006; accepted 26 April 2006
Available online 30 August 2006

**Abstract**

The correlation between dynamic magnetic domain formation and dynamic magnetization loss is studied in nanocrystalline FeCuNbSiB tape wound cores with different strengths of transverse field-induced anisotropy. A significant excess loss component is measured, in particular for high induction levels. The excess loss cannot be explained by homogeneous magnetization rotation, the ideal magnetization process for a transverse field-induced anisotropy. In fact, dynamic domain observation reveals inhomogeneous rotation of magnetization, wall displacement processes, and domain nucleation besides homogeneous rotation. Domain refinement is accordingly observed with increasing frequency. The domain width is smallest for cores with weak induced anisotropy, where excess loss is the lowest. In these cores, surface roughness yields residual domains, which persist at field strengths above the inductively measured saturation field.


*Keywords:* Kerr–Faraday magnetometry; Nanocrystalline materials; Magnetic domain; Dynamic phenomena; Magnetization loss

## 1. Introduction

Soft magnetic FeCuNbSiB nanocrystalline ribbons were first reported by Yoshizawa et al. [1]. Vanishing magnetostriction, low coercivity, and a saturation induction of typically 1.2–1.3 T result in superior soft magnetic properties of FeCuNbSiB alloys. It is well known that the magnetization curve of nanocrystalline ribbons can be varied by a magnetic anisotropy induced by a magnetic field [1,2] or creep annealing [3].

Nanocrystalline tape wound cores are favorable for applications at elevated frequencies up to 100 kHz [4], because the small ribbon thickness of around 20 μm and the high electrical resistivity of 115 μΩ cm minimize eddy current loss. As in other soft magnetic materials, the dynamic loss in nanocrystalline ribbons can be separated into classical eddy current loss and excess loss [5]. The excess loss originates from micro-eddy currents surrounding the moving domain walls and, hence, is of particular significance for longitudinal field annealed cores where the magnetization process is governed by domain wall displacements (cf. Ref. [6]). In contrast, excess loss should be absent for homogeneous magnetization processes. The latter is the case for transverse anisotropies, where the magnetization process is governed in a simple model by the rotation of the magnetization vector towards the applied field. However, Kerr microscopy observations have revealed wall displacement processes, inhomogeneous rotations, domain nucleation, and domain splitting besides homogeneous rotations in nanocrystalline ribbons with transverse field-induced anisotropy [7]. Such magnetic inhomogeneities, of course, cause a corresponding excess loss contribution in transverse field annealed material as, for example, reported by Ferrara et al. [8]. Excess loss

* Corresponding author. Tel.: +49 3514659245; fax: +49 3514659241.
*E-mail address:* s.flohrer@ifw-dresden.de (S. Flohrer).

1359-6454/$30.00 
doi:10.1016/j.actamat.2006.04.040

has also been observed in transverse field annealed amorphous ribbons [9], although these materials tend to reveal a more homogeneous magnetization process than nanocrystalline alloys because the average random local anisotropy is vanishing (cf. Ref. [7]). Interestingly, as also shown in Ref. [9], the excess loss contribution increases with increasing induced anisotropy, although the fractional contribution of homogeneous to inhomogeneous magnetization process increases at the same time.

The objective of the present paper is to give a more detailed characterization and a deeper understanding of the excess loss contribution in transverse field annealed nanocrystalline cores. For this purpose we have investigated the magnetization process of nanocrystalline cores with different strengths of transverse field-induced anisotropy for frequencies up to 10 kHz by means of dynamic Kerr microscopy in combination with simultaneous loss and hysteresis loop measurements.

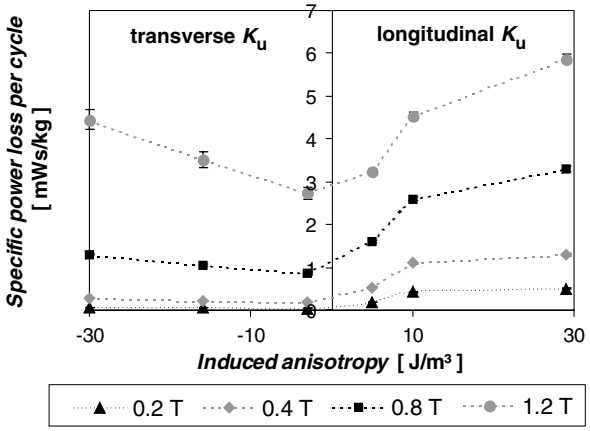


Fig. 1. Specific power loss per cycle at a frequency of 10 kHz and various peak induction levels (0.2–1.2 T) for nanocrystalline tape wound cores with different strengths of field-induced anisotropy $K_u$. Negative values of the induced anisotropy mark transverse $K_u$, positive values longitudinal $K_u$.

## 2. Experimental

Nanocrystalline toroidal tape wound cores of $Fe_{73-x}Cu_1Nb_3Si_{16+x}B_7$ ($x = 0$ and 1.5) with a ribbon thickness of 20 μm and a width of about 20 mm were studied. The initial material was produced as an amorphous ribbon via rapid solidification technology and wound to toroidal cores in the final dimensions. A subsequent annealing treatment was performed to achieve the nanocrystalline state. During annealing, a saturating transverse magnetic field was applied for appropriate times and temperatures to induce an anisotropy of desired strength [6]. A relatively strong induced anisotropy constant $K_u$ of about 30 J/m$^3$ was achieved for $x = 0$ by applying the magnetic field during the entire annealing at 570 °C for 0.5 h. An anisotropy of moderate strength ($K_u \approx 16$ J/m$^3$) was induced for $x = 1.5$ by field annealing at 580 °C for 0.5 h. A third core with $x = 0$ was transverse field annealed for 3 h at 420 °C after having been crystallized in a longitudinal magnetic field at 570 °C for 0.5 h. This annealing condition resulted in a significantly smaller $K_u$ of about 3 J/m$^3$. For the comparison in Fig. 1, loss measurements were also performed on cores with longitudinal $K_u$ [10]. The saturation magnetization of the material studied was 1.2 T [11].

The domain structure was observed using Kerr microscopy with a standard optical wide-field polarization microscope. All images shown are difference images obtained by subtracting the non-magnetic background [12]. The microscope was extended with a gated image intensifier for stroboscopic imaging. Details of the experimental setup are given elsewhere [10]. The tape wound cores were magnetized along their circumferential direction. Domain observations and simultaneous loss measurements were performed from the quasi-static case up to 10 kHz. A nearly sinusoidal induction waveform was obtained by digital feedback [13]. The stroboscopic images were obtained with an exposure time of one-hundredth of the magnetic field period. To obtain sufficient contrast, intensity accumulation of several thousand single images was necessary for every image shown. Because of the intensity accumulation, only reproducible magnetization processes can be observed.

## 3. Results and discussion

The dependence of the specific power loss per cycle on the induction amplitude of nanocrystalline tape wound cores is shown in Fig. 1 for transverse (negative values) and longitudinal (positive values) field-induced anisotropy $K_u$ at a frequency of 10 kHz. At low induction amplitudes of 0.2 and 0.4 T, the total loss is much smaller in cores with transverse $K_u$ compared to those with longitudinal $K_u$. Furthermore, the total loss does not depend considerably on the strength of transverse $K_u$, if the induction amplitude is small. However, magnetizing close to saturation reveals a significant increase in the total loss with increasing strength of transverse $K_u$. The difference in the total loss of the cores is due to different excess losses, because the hysteresis loss is very small (below 0.4 mW s/kg at a maximum induction of 1.2 T) and the classical eddy current loss is similar for all cores. To study the origin of excess loss depending on the strength of transverse $K_u$, simultaneous stroboscopic domain observation and measurement of the dynamic loss were performed by magnetizing close to saturation. The correlation of excess loss and dynamic magnetization process in cores with different strengths of longitudinal $K_u$ is given in Ref. [10].

The magnetization curves of the nanocrystalline cores with three different strengths of transverse $K_u$ are shown in Fig. 2. Flat hysteresis loops with a constant permeability are obtained over a wide field range. The quasi-static hysteresis loops, in contrast to the data of Ferrara et al. [8], reveal a high degree of linearity and hardly show any appreciable hysteresis effect ($H_c < 1$ A/m), both indicating magnetization rotation as the dominant magnetization

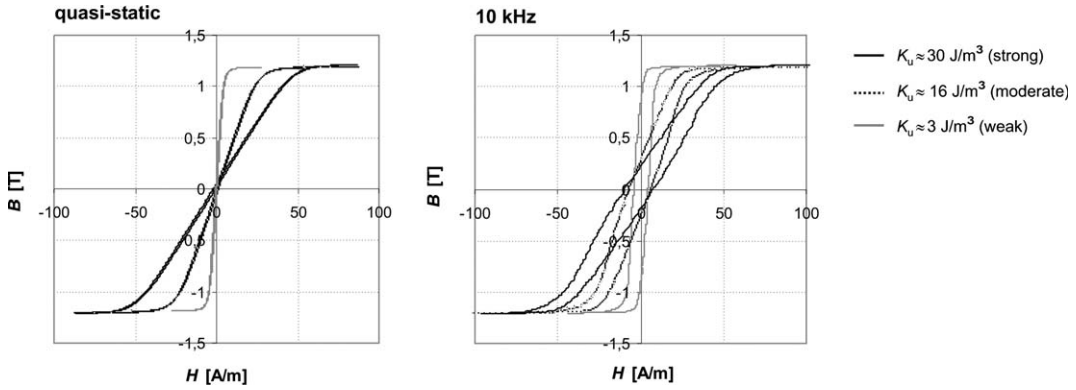


Fig. 2. Hysteresis loops of three nanocrystalline tape wound cores with different strengths of transverse field-induced anisotropy $K_u$ at very low frequencies (left) and at 10 kHz (right).

process. The loop area increases significantly with increasing frequency, because of the induced eddy currents.

The specific power loss per cycle up to 10 kHz is depicted in Fig. 3 for magnetizing to a peak induction of 1.2 T. The method of loss separation [5] is applied to analyze the dynamic loss. It is dominated by the excess loss component, which becomes augmented with increasing $K_u$. The excess loss per cycle is typically proportional to the square root of the frequency due to a dynamic increase of active domains [14]. This dependency is obtained for all cores (Fig. 4) above a frequency of a few hertz. There is a deviation from linearity at low frequencies which has been previously reported for non-oriented and grain-oriented Fe–Si by Barbisio et al. [15].

Direct observation of the dynamic increase in the number of domains is shown by time-resolved Kerr images of the cores with strong and weak $K_u$ in Fig. 5. The images were obtained around the coercive field and were recorded simultaneously with the magnetization loss measurements of Fig. 3. The domain boundaries appear sharp, indicating repeatability of the magnetization processes. During magnetization at a frequency of 50 Hz, regular wide domains are formed, separated by 180° walls. This domain structure is typical of nanocrystalline FeCuNbSiB ribbons with a uniaxial induced anisotropy [7,16]. The domain width is smaller at lower $K_u$, which is also the case during quasi-static remagnetization. The static domain width is proportional to the square root of $K_u$ according to the minimum of the total magnetic Gibbs free energy [17]. Domain refinement is clearly visible for both strengths of $K_u$ with increasing frequency.

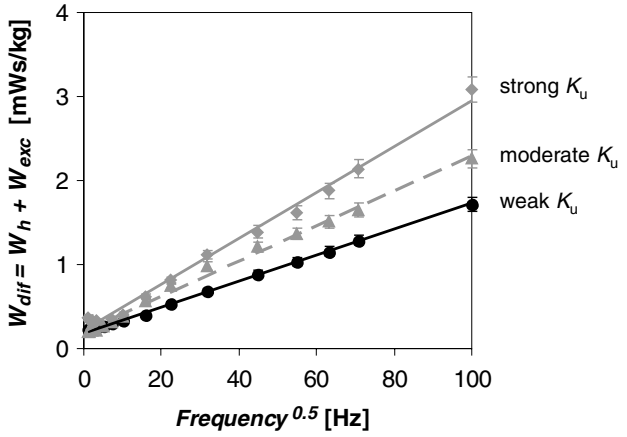


Fig. 4. Sum $W_{dif}$ of hysteresis loss $W_h$ and excess loss per cycle $W_{exc}$ vs. square root of frequency deviates from the typical linear behavior only at low frequencies.

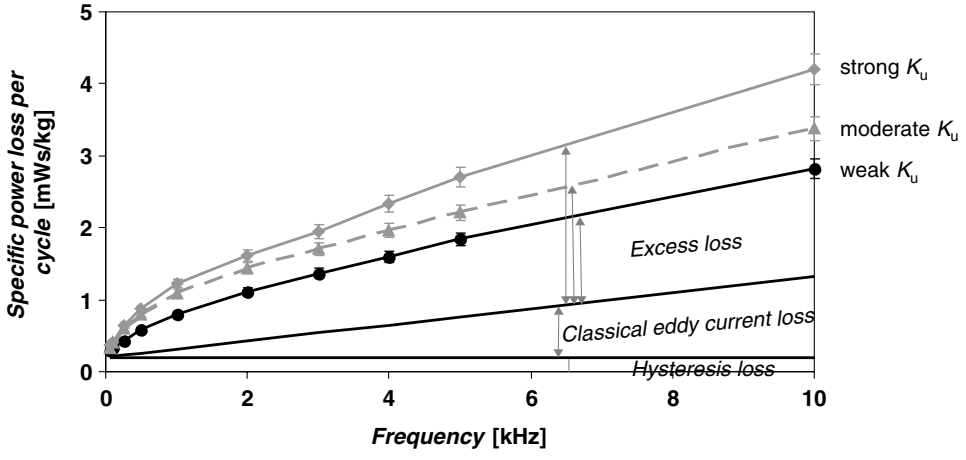


Fig. 3. Specific power loss per cycle vs. frequency. The excess loss component increases with increasing $K_u$.

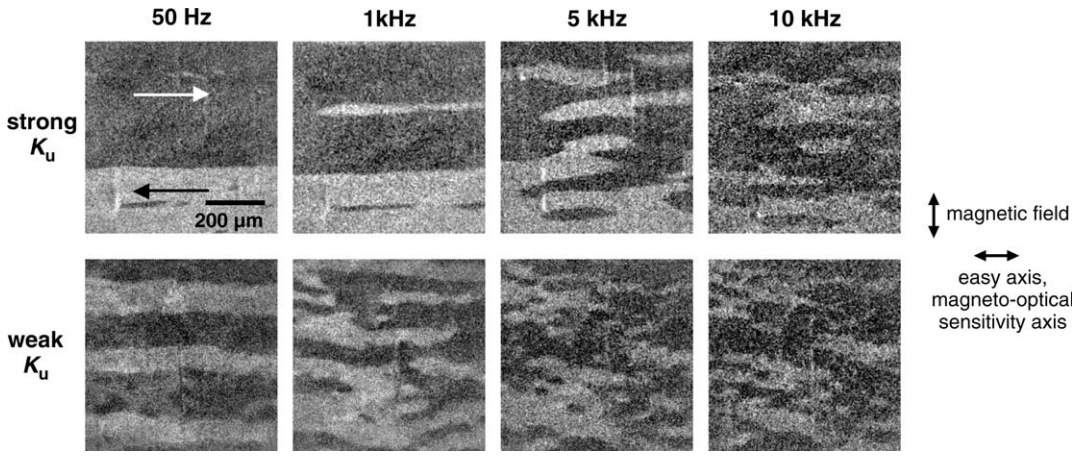


Fig. 5. Domain refinement with increasing frequency of nanocrystalline cores with strong and weak $K_u$. Arrows indicate the magnetization direction.

The average number of domain walls, observed on seven different sample spots for each case, is plotted in Fig. 6. The domain wall number is obtained by counting the number of intersections between dark and bright contrast in the Kerr images along line scans transverse to the magnetic easy axis. The counted number is scaled up in Fig. 6 to the whole circumference of the outermost ribbon of the core. Of course, only a small part of the complete core volume is observed using Kerr microscopy, and the shape of the domains changes from elongated wide domains to irregular domains with increasing frequency. Nevertheless, the data indicate a nearly linear increase of the domain wall number with the square root of the frequency. The largest number of domain walls is obtained at weak $K_u$, where excess loss is the smallest.

Domain refinement is a typical phenomenon leading to less than linear increase of the excess loss per cycle vs. frequency in soft magnets with induced anisotropy along the field axis, where domain wall displacement processes govern remagnetization. In our case of transverse $K_u$, domain wall displacements might be activated by wall segments that are locally inclined relative to the macroscopic induced easy axis. Such misalignment may be caused by stray fields due to surface roughness and demagnetizing effects at the edges.

Fig. 7 gives an insight into the magnetization process of the core with strong $K_u$ in a decreasing magnetic field starting at saturation for the quasi-static case, 500 Hz and 5 kHz. The images at 500 Hz and 5 kHz were obtained with the stroboscopic technique. Homogeneous magnetization rotation is the dominant magnetization process. As predicted from the occurrence of excess loss, slight wall displacement processes can in fact be observed in the images. Domain contrast is still present above the inductively measured "technical" saturation field $H_s$ of around 80 A/m.

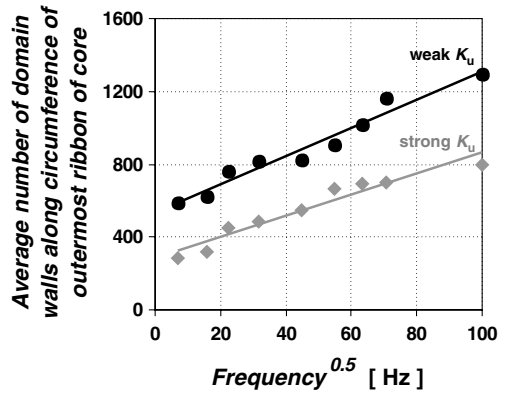


Fig. 6. Average number of surface domain walls along core circumference vs. square root of the frequency.

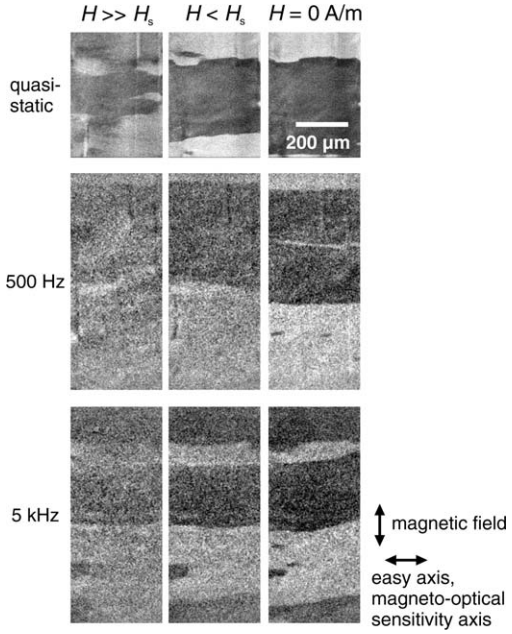


Fig. 7. Magnetization process of the core with strong $K_u$ in a decreasing magnetic field for quasi-static remagnetization, at 500 Hz and at 5 kHz. Homogeneous rotation dominates the magnetization process. Slight wall displacements are also visible.

The quasi-static and the dynamic magnetization process of the core with weak $K_u$ in a decreasing magnetic field is presented in Fig. 8. Above $H_s$ (~20 A/m), magneto-optical contrast is visible as stripe-like magnetization fluctuations perpendicular to the magnetic field direction. The fluctuations (residual domains) become more distinct when the applied magnetic field decreases and, for $H < H_s$, finally rearrange into the wide laminar domains characteristic of the transverse anisotropy.

To study the origin of the residual domains in more detail, their behavior in a rotating magnetic field was investigated (Fig. 9). The experiments were performed on single ribbon pieces (with a length of some millimeters) of the core with weak $K_u$, which were magnetized in a rotatable electromagnet. The low-angle domains persist up to strong magnetic fields of several tens of kA/m, far beyond the "technical" saturation field $H_s$ and only disappear for applied fields beyond about 50 kA/m. The residual domains are aligned perpendicular to the applied field, even when the field is rotated (see Fig. 9, second line). Simplified sketches of stripe-like domains are shown in the right column of Fig. 9. The arrows indicate the direction of magnetization. The residual domains invert their magneto-optical contrast if the direction of the applied field is reversed, without changing their shape (not shown).

The stripe-like modulation of magnetization with a texture orthogonal to the average magnetization resembles the ripple structure in sputtered magnetic films. Ripples reflect the irregular polycrystalline nature of the films and can be described as the reaction to a statistical perturbation by the crystal anisotropy of the individual grains. In the case of nanocrystalline ribbons (which may be considered as bulk material), a patchy modulation of magnetization, rather than a stripe-like modulation, is observed in the multidomain state [7]. The patches were interpreted by Herzer [18] as exchange volumes within the framework of the random anisotropy model. In Ref. [19], it was shown that the patchy modulation transforms into ripple by thinning the ribbons into the micrometer regime. This observation indicates that ripple and patches are both caused by the nanocrystalline microstructure in each case. However, there is also a statistical perturbation caused by stray field effects at the ribbon surface due to roughness. This perturbation

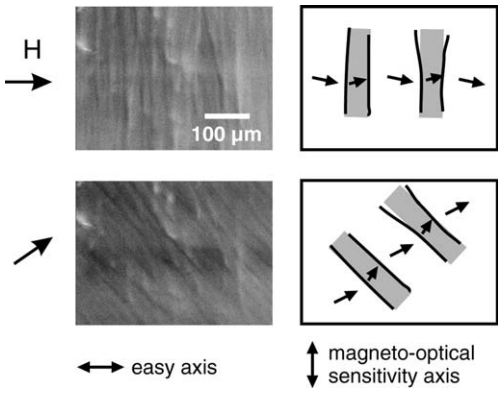


Fig. 9. Domain images and corresponding sketches of the stripe-like domains at an applied field of 20 kA/m in different directions. The domains are aligned perpendicular to the applied field.

may cause the stripe-like modulation described here. No theory of such a "stray-field-induced ripple" is available. Like in the case of "true" ripple in films, the orthogonal texture of the modulation is caused by the stray-field energy that is smaller for longitudinal rather than transverse modulation [16].

Fig. 10 shows the formation of residual domains after mechanically polishing either the air-side (Fig. 10a) or the wheel-side (Figs. 10b and c) of the nanocrystalline ribbon with weak $K_u$ with Matermed 2 suspension from Buehler. While polishing the air-side does not obviously influence the residual domain structure, polishing the wheel-side reduces the magneto-optical contrast of the residual domains significantly. The field-induced anisotropy is still present after polishing and yields wide domains along the easy axis at zero field in all cases. Strong polishing of the wheel-side as in Fig. 10c leads to a complete disappearance of the residual domains on the air-side.

The results after polishing clearly indicate that in the present case the ripple arises from surface roughness and not from the nanocrystalline microstructure. This conclusion is also supported by the fact that we as well as Amalou et al. [20] find similar high-field domains for amorphous ribbons, where the average random anisotropy contribution of the structure is orders of magnitude lower (cf. Ref. [18]). The formation of the residual domains

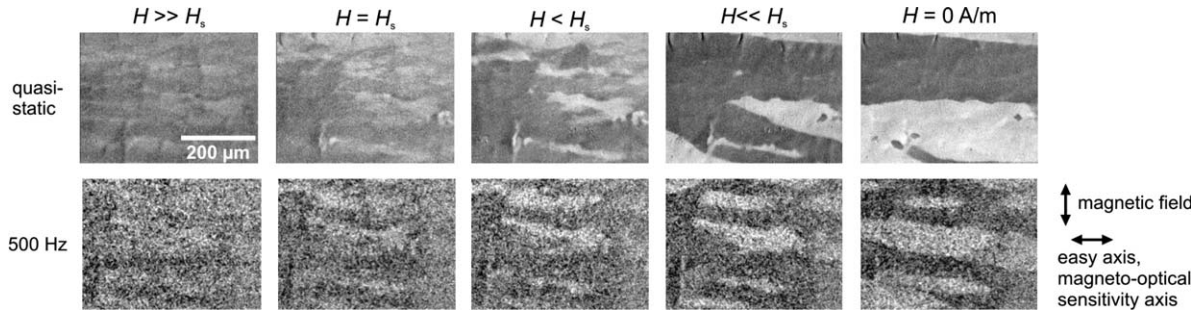


Fig. 8. Magnetization process of the core with weak $K_u$ in a decreasing magnetic field for the quasi-static case and at 500 Hz. The wide domains arise at stripe-like residual domains that persist far beyond the "technical" saturation field $H_s$.

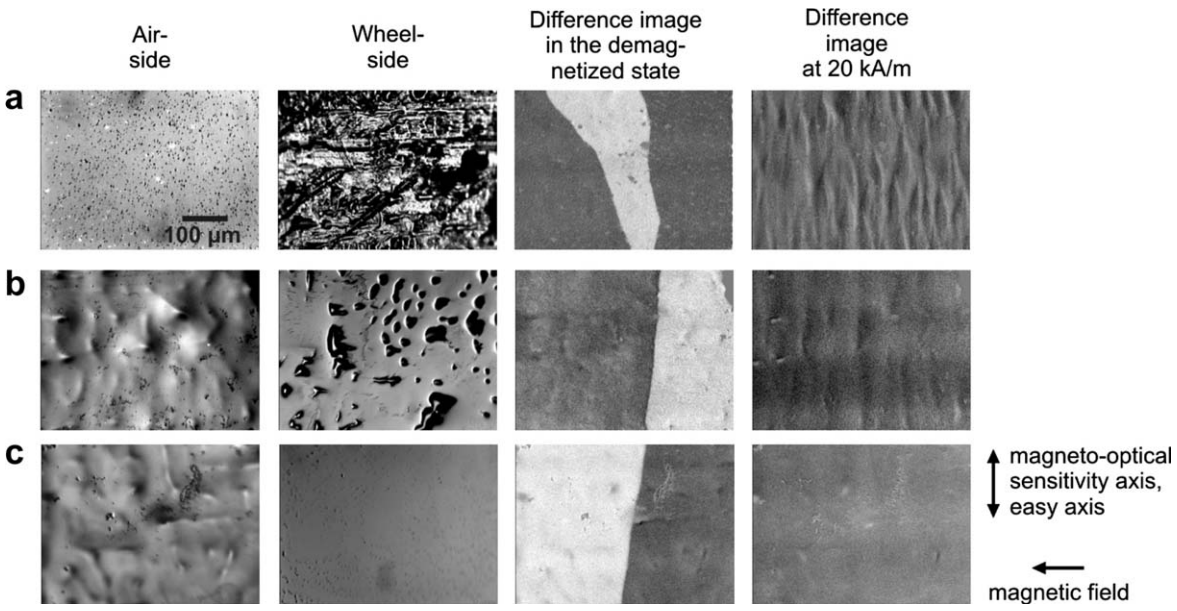


Fig. 10. Appearance of stripe-like domains in the difference image at high field strengths depends on the roughness of the wheel-side. The difference images are obtained at the indicated spot of the air-side: (a) unpolished wheel-side, polished air-side; (b) slightly polished wheel-side, unpolished air-side; and (c) strong polished wheel-side, unpolished air-side.

illustrates why the fully ferromagnetically saturated state in near-zero magnetostrictive nanocrystalline and Co-based amorphous ribbons with large surface roughness [21] needs relatively high applied magnetic fields of a couple of tens of kA/m.

## 4. Conclusions

The dynamic magnetization process in nanocrystalline FeCuNbSiB tape wound cores with transverse field-induced anisotropy has been studied using stroboscopic Kerr microscopy and simultaneous loss measurements. The cores reveal significant excess loss at high induction levels, where the material was driven into magnetic saturation. As demonstrated by domain observations, these excess losses are associated with inhomogeneous magnetization processes in addition to the expected magnetization rotation process. The excess loss contribution increases with increasing strength of the induced anisotropy. The lower excess loss in cores with weak induced anisotropy is ascribed to a larger number of active domain walls compared to cores with higher induced anisotropy. It was demonstrated that the surface roughness on the wheel-side of the ribbons causes a ripple-like domain structure that provides an important contribution for the nucleation of reversed domains.

## Acknowledgements

We thank S. Schinnerling (IFW Dresden) and S. Pofahl (IFW Dresden) for sample preparation.

## References

[1] Yoshizawa Y, Oguma S, Yamauchi K. J Appl Phys 1988;64:6044.
[2] Yoshizawa Y, Yamauchi K. IEEE Trans Magn 1989;25:3324.
[3] Kraus L, Závěta K, Heczko O, Duhaj P, Vlasák G, Schneider J. J Magn Magn Mater 1992;112:275.
[4] Petzold J. J Magn Magn Mater 2002;242–245:84.
[5] Bertotti G. Hysteresis in magnetism. San Diego (CA): Academic Press; 1998.
[6] Herzer G. In: Buschow KHJ, editor. Handbook of magnetic materials, vol. 10. Amsterdam: Elsevier Science; 1997. p. 415.
[7] Flohrer S, Schäfer R, Polak C, Herzer G. Acta Mater 2005;53:2937.
[8] Ferrara E, De Luigi C, Beatrice C, Appino C, Fiorillo F. J Magn Magn Mater 2000;215–216:466.
[9] Beatrice C, Appino C, Ferrara E, Fiorillo F. J Magn Magn Mater 1996;160:302.
[10] Flohrer S, Schäfer R, McCord J, Roth S, Schultz L, Herzer G. Acta Mater 2006;54:3253.
[11] Data specification, Vacuumschmelze GmbH Co. KG, Hanau, Germany.
[12] Schmidt F, Rave W, Hubert A. IEEE Trans Magn 1985;21:1596.
[13] Bertotti G, Ferrara E, Fiorillo F, Pasquale M. J Appl Phys 1993;73:5375.
[14] Bertotti G. IEEE Trans Magn 1988;24:621.
[15] Barbisio E, Fiorillo F, Ragusa C. IEEE Trans Magn 2004;40:1810.
[16] Hubert A, Schäfer R. Magnetic domains. The analysis of magnetic microstructures. Berlin: Springer; 1998. p. 453,547.
[17] Kronmüller H, Moser M, Reininger T. An Fis B 1990;86:1.
[18] Herzer G. J Magn Magn Mater 2005;294:99.
[19] Schäfer R. J Magn Magn Mater 2000;215–216:652.
[20] Amalou F, Gijs MAM. J Appl Phys 2001;90:3466.
[21] Herzer G. An Fis B 1990;86:64.